Published in final edited form as:
J Mol Biol. 2008 October 3; 382(2): 312–326. doi:10.1016/j.jmb.2008.07.012.

Influence of DNA End Structure on the Mechanism of Initiation of DNA Unwinding by the *E. coli* RecBCD and RecBC Helicases

Colin G. Wu and **Timothy M. Lohman***
Department of Biochemistry and Molecular Biophysics Washington University School of Medicine 660 S. Euclid Avenue, Box 8231 Saint Louis, MO 63110

Abstract

E. coli RecBCD is a bipolar DNA helicase possessing two motor subunits (RecB, a 3' to 5' translocase and RecD, a 5' to 3' translocase), that is involved in the major pathway of recombinational repair. Previous studies indicated that the minimal kinetic mechanism needed to describe the ATP-dependent unwinding of blunt-ended DNA by RecBCD *in vitro* is a sequential *n*-step mechanism with two to three additional kinetic steps prior to initiating DNA unwinding. Since RecBCD can "melt-out" ~ six bp upon binding to the end of a blunt-ended DNA duplex in a Mg^{2+}-dependent but ATP-independent reaction, we have investigated the effects of non-complementary single-stranded (ss) DNA tails (3'-$(dT)_6$ and 5'-$(dT)_6$ or 5'-$(dT)_{10}$) on the mechanism of RecBCD and RecBC unwinding of duplex DNA using rapid kinetic methods. As with blunt-ended DNA, RecBCD unwinding of DNA possessing 3'-$(dT)_6$ and 5'-$(dT)_6$ non-complementary ssDNA tails is well described by a sequential *n*-step mechanism with the same unwinding rate (mk_U = 774 ± 16 bp s^{-1}) and kinetic step-size (m = 3.3 ± 1.3 bp), yet two to three additional kinetic steps are still required prior to initiation of DNA unwinding (k_C = 45 ± 2 s^{-1}). However, when the non-complementary 5'-ssDNA tail is extended to ten nucleotides (5'-$(dT)_{10}$ and 3'-$(dT)_6$), the DNA end structure for which RecBCD displays optimal binding affinity, the additional kinetic steps are no longer needed, although a slightly slower unwinding rate (mk_U = 538 ± 24 bp s^{-1}) is observed with a similar kinetic step-size (m = 3.9 ± 0.5 bp). The RecBC DNA helicase (without the RecD subunit) does not initiate unwinding efficiently from a blunt DNA end. However, RecBC does initiate well from a DNA end possessing non-complementary twin 5'- dT_6 and 3'-dT_6 tails, and unwinding can be described by a simple uniform *n*-step sequential scheme, without the need of the additional k_C initiation steps, with a similar kinetic step size (m = 4.4 ± 1.7 bp), and unwinding rate (mk_{obs} = 396 ± 15 bp s^{-1}). These results suggest that the additional kinetic steps with rate constant k_C required for RecBCD to initiate unwinding of blunt-ended and twin (dT_6)–tailed DNA reflect processes needed to engage the RecD motor with the 5' ssDNA.

Introduction

DNA helicases are a diverse class of nucleic acid motor proteins that function by coupling the binding and hydrolysis of 5'-nucleoside triphosphate (NTP) to translocation along the DNA filament and unwinding of duplex DNA in order to form the single-stranded (ss)

*Address correspondence to: Timothy M. Lohman Department of Biochemistry and Molecular Biophysics Washington University School of Medicine 660 S. Euclid Avenue, Box 8231 Saint Louis, MO 63110 (314)-362-4393 (314)-362-7183 (Fax) lohman@biochem.wustl.edu.

intermediates required for DNA replication, recombination, and repair[1; 2; 3; 4; 5; 6; 7]. Some helicases can also displace other proteins from the nucleic acid[8; 9; 10; 11; 12]. Because helicase function is involved in all aspects of DNA metabolism, defects in human helicases can give rise to genetic disorders such as Bloom's syndrome, Werner's syndrome, Rothmund-Thomson's syndrome, xeroderma pigmentosum, and others as well[13; 14; 15; 16].

In *E. coli*, the RecBCD pathway is the major pathway for homologous recombination and repair of double-stranded (ds) DNA breaks. RecBCD is an essential DNA helicase for this pathway and is composed of the RecB (134 kDa), RecC (129 kDa), and RecD (67 kDa) polypeptides[17; 18; 19]. This heterotrimeric enzyme processes dsDNA breaks with its ds and ssDNA exonuclease, ssDNA endonuclease, DNA dependent ATPase, and helicase activities, which are regulated by the crossover hotspot instigator (chi) regulatory sequence (5'-GCTGGTGG-3')[20; 21; 22; 23]. RecBCD first binds to the damaged induced dsDNA break at a blunt or nearly blunt end, and then unwinds the duplex in an ATP dependent reaction. During DNA unwinding, its nuclease activity preferentially degrades the 3' terminating DNA strand while cleaving the 5' terminating strand infrequently[24; 25]. These activities are modified when RecBCD recognizes a chi sequence, whereupon RecBCD first pauses and then continues to unwind DNA with a reduced rate[26; 27; 28]. Furthermore, the nuclease activity is altered such that it acts instead on the 5' terminating strand preferentially. This generates a 3' ssDNA overhang onto which RecBCD loads the RecA protein[29] and the resulting RecA coated DNA filament forms a joint molecule with a homologous piece of DNA and initiates recombinational repair of the nucleic acid.

RecB and RecD are both superfamily-1 (SF1) helicases/translocases[30], with opposite ssDNA translocation directionalities. Although the two motor subunits have opposite ssDNA translocation polarities (RecB is a 3' to 5' translocase, while RecD is a 5' to 3' translocase), they function in unison to unwind dsDNA in the same net direction within the RecBCD heterotrimer by interacting with opposite strands of the DNA end[31; 32]. Interestingly, the RecBC enzyme, lacking the RecD subunit, is still a functional helicase. Both RecBCD and RecBC are processive helicases[26; 33; 34] that form stable heterotrimers and heterodimers, respectively in solution[35; 36; 37].

Equilibrium binding studies have indicated that RecBCD binds optimally to DNA ends possessing non-complementary 5'-$(dT)_{10}$ and 3'-$(dT)_6$ ssDNA tails while the RecBC binds optimally to DNA ends with 5'-$(dT)_6$ and 3'-$(dT)_6$ tails[37]. These results indicate that both the RecBCD and RecBC helicases are able to “melt-out” six base pairs simply upon binding to a blunt-ended duplex in a Mg^{2+}-dependent, but ATP-independent reaction[38]. In a crystal structure of a RecBCD-DNA complex, the last four base pairs are observed to be melted even though the complex was crystallized in presence of Ca^{2+} [39]. Furthermore, the equilibrium binding studies suggest that an additional four nucleotides in the non-complementary 5' ssDNA tail is needed to facilitate interactions with the RecD subunit[37].

Lucius et al.[40; 41; 42] previously determined a minimal kinetic mechanism by which RecBCD unwinds blunt-ended DNA duplexes *in vitro* using rapid kinetic methods under single-turnover conditions. A simple uniform *n*-step sequential scheme was not able to describe the time courses for RecBCD unwinding of blunt-ended DNA. In fact, the minimal kinetic mechanism required two to three additional kinetic steps, which made determination of the average DNA unwinding kinetic step-size more difficult, although a well constrained kinetic step-size of (3.9 ± 0.5) bp was determined that was independent of ATP concentration and temperature[40]. The number (two to three) of these additional steps was found to be independent of DNA duplex length, suggesting that these steps are not associated with the repeated cycles of DNA unwinding, and likely precede or occur at the early stages of DNA unwinding[42]. Here, we examine the effects of non-complementary 3'-

and 5'-ss-DNA tails on the mechanism by which RecBCD and RecBC initiate and processively unwind DNA in order to probe the role of RecD in the initiation of DNA unwinding.

Results

The DNA substrates used in this study are shown schematically in Figure 1 and the sequences of the individual DNA strands are given in Table 1. They consist of a DNA duplex containing two nicks with a hairpin structure on one end, while the other end possessing non-complementary ssDNA tails ($(dT)_n$), which forms the site at which RecBCD or RecBC will initiate unwinding. With the exception of the DNA substrate used in the experiments shown in Figure 3 which possesses a blunt-end, the 3' ssDNA tail length is six nucleotides ((dT_6)), while the 5'ssDNA length is either six ((dT_6)) or ten ((dT_{10})) nucleotides. For the chemical quenched-flow unwinding experiments (see Figure 2A), strand "A" is radiolabeled with ^{32}P on its 5' end (denoted as an asterisk in Figure 1A). Displacement of the radioactively labeled DNA is used to monitor DNA unwinding in a discontinuous assay (see Materials and Methods). For the stopped-flow fluorescence experiments (see Figure 2B), Cy3 and Cy5 fluorophores are positioned on either side of a nick (see Figure 1B) and changes in Cy3 and Cy5 fluorescence resulting from changes in fluorescence resonance energy transfer (FRET) are used to monitor DNA unwinding. Both assays are "a'll or none" assays since DNA unwinding is not detected until duplex "A" (see Figures 1 and 2) is fully unwound; however, information on intermediate species present during unwinding can be obtained by analyzing a series of unwinding experiments performed as a function of DNA duplex length[43; 44].

RecBC initiates DNA unwinding poorly from a blunt DNA end

Single-turnover chemical quenched-flow kinetic studies were performed as described in Materials and Methods[41]. The kinetics of RecBC and RecBCD-catalyzed unwinding of a 24 bp blunt ended DNA (Substrate I without the non-complementary $(dT)_n$ tails) used in our previous studies[42], are shown in Figure 3. Whereas RecBCD is able to initiate unwinding rapidly from a blunt DNA end, much less unwinding is catalyzed by RecBC. These single turnover kinetic experiments were performed using the same pre-incubation concentrations of RecBCD and RecBC (40 nM). We note that in a multiple turnover experiment our preparation of RecBC enzyme shows similar DNA unwinding behavior with a blunt ended DNA substrate as reported previously[45] (see Materials and Methods). One possibility is that the much lower amplitude of DNA unwinding by RecBC may result from a weaker affinity of RecBC for DNA blunt ends compared with RecBCD[37]. However, based on our estimate of $\sim 2 \times 10^7\ M^{-1}$ for the equilibrium constant for RecBC binding to a blunt end under these conditions[37], ~95% of the DNA ends should be bound with RecBC. Consistent with this conclusion, we observe no difference in the amplitude of unwinding when these experiments are performed using a ten-fold higher pre-incubation concentration (400 nM) of RecBC. This suggests that the majority of the RecBC enzyme must be bound in a non-productive mode to a blunt duplex end. Previous studies have shown that RecBC binds with highest affinity to DNA ends possessing non-complementary 5'-(dT_6) and 3'-(dT_6) ssDNA tails, while RecBCD binds optimally to DNA ends with non-complementary 5'-(dT_{10}) and 3'-(dT_6) ssDNA tails[37]. Based on this, we examined the effect of such non-complementary ssDNA tails on the kinetics and mechanism of DNA unwinding by both RecBC and RecBCD enzymes.

Minimal kinetic mechanism of RecBC-catalyzed DNA unwinding

We examined RecBC-catalyzed unwinding of a series of DNA duplexes possessing non-complementary 5'-$(dT)_6$ and 3'-$(dT)_6$ ssDNA tails using rapid chemical quenched-flow and

stopped-flow fluorescence techniques (see Materials and Methods). Quenched-flow experiments were performed with DNA substrates of the type shown in Figure 1A with duplex region "A" varying in length ((24, 30, 40, 48, 60 bp (Substrates I, III, V, VII, and XI)). Three independent sets of measurements were performed with each duplex length. The average time courses are plotted in Figure 4A and were analyzed by global non-linear least squares (NLLS) analysis using Scheme 1 (eq. (2)). The solid curves in Figure 4A are simulated time courses using eq. (2) and the best fit parameters (m = 4.4 ± 1.7 bp, k_{obs} = 90 ± 25 s^{-1}, mk_{obs} = 396 ± 15 bp/s, k_{NP} = 1.7 ± 0.5 s^{-1}). It is clear from the data in Figure 4A that RecBC is able to initiate DNA unwinding with much higher efficiency from a DNA end possessing the non-complementary 5'-$(dT)_6$ and 3'-$(dT)_6$ ssDNA tails than from a blunt DNA end (see Figure 3).

As observed previously for RecBCD-catalyzed unwinding of blunt-ended DNA duplexes, the time courses all display a lag phase. This lag phase results from the fact that the assays used are "all or none" and RecBC must proceed through a series of sequential kinetic steps (with similar rate constants, k_U) in order to fully unwind each duplex. The number of these unwinding steps, and thus the duration of the lag phase, increases with duplex length. In addition to this lag phase, we also observe a slower unwinding phase that is much smaller in amplitude. As discussed previously[41], we attribute these two phases to DNA unwinding from two populations of initially bound RecBC-DNA complexes. One population of RecBC is bound in a productive mode that can initiate DNA unwinding rapidly upon the addition of ATP, while the other population of RecBC is bound in a non-productive manner that must first undergo a slow isomerization, with rate constant k_{NP}, to form productive complexes before DNA unwinding can initiate.

Since RecBC-catalyzed unwinding of duplex DNA occurs via multiple (n) repeated steps, with rate-limiting rate constant, k_U, the number of DNA unwinding steps, n, is expected to increase in direct proportion to the DNA duplex length L. In fact, Figure 4B shows that the values of n determined from NLLS fitting of the data to the simple Scheme 1 are directly proportional to L. A summary of the kinetic parameters obtained from the NLLS fitting is given in Table 2. In Scheme 1, productively bound RecBC can unwind the DNA in uniform steps with rate constant k_U. The average kinetic step-size, m, is defined as the average number of bp that are unwound between such two successive rate limiting steps. Based on the NLLS fitting of the data in Figure 4A, RecBC has an average kinetic step-size of 4.4 ± 1.7 bp for DNA unwinding, with a stepping rate of 90 ± 25 sec^{-1}, resulting in a macroscopic unwinding rate of mk_{obs} = 396 ± 15 bp/sec.

We also examined the kinetics of RecBC-catalyzed unwinding of DNA duplexes possessing non-complementary twin 3'-$(dT)_6$ and 5'-$(dT)_6$ ssDNA tails using a stopped-flow fluorescence technique described previously[42]. These experiments were performed using a series of DNA substrates of the type shown in Figure 1B with duplex region "A" varying in length (24, 29, 37, 40, 43, 48, 53, 60 bp (Substrates I, II, IV, V, VI, VII, VIII, IX)). DNA unwinding was monitored by the loss of FRET between a Cy3 donor fluorophore and a Cy5 acceptor fluorophore. As indicated in Figure 2B, the stopped-flow assay is also "all or none". When the DNA duplex is fully unwound and the labeled DNA strands are displaced, the two dyes become separated and thus Cy3 fluorescence increases while there is a concomitant loss in Cy5 fluorescence due to the loss of energy transfer from Cy3 to Cy5.

The time courses monitoring the increase in Cy3 fluorescence (averages of three independent measurements) are plotted in Figure 5A and the solid curves are global NLLS fits to the simple Scheme 1 (eq. 2) (m = 4.4 ± 0.1 bp, k_{obs} = 79 ± 11 s^{-1}, mk_{obs} = 348 ± 5 bp/s, k_{NP} = 1.1 ± 0.1 s^{-1}). These time courses are also well-described by Scheme 1 and the number of unwinding steps, n, determined from the data fitting is directly proportional to

duplex length, *L* (Figure 5B). The Cy5 fluorescence time courses (see Supplementary Figure 1), which are exactly anti-correlated with the Cy3 fluorescence time courses, can be analyzed as well using Scheme 1 (eq. 2), yielding identical kinetic parameters. It is interesting to note that in previous RecBCD stopped-flow unwinding studies[42], the resulting Cy5 fluorescence time courses showed a more complex time course that was not fully anti-correlated with the Cy3 fluorescence time course. This deviation[42] was attributed to the RecD subunit, which translocates along the 5' ending DNA strand in the 5' to 3' direction, ultimately contacting the Cy3 fluorophore at the nick resulting in an enhancement of the Cy3 fluorescence. This increase in Cy3 fluorescence was then transferred via FRET to the Cy5 fluorophore before the strands are separated resulting in an additional increase in Cy5 fluorescence. This effect is not observed with the RecBC enzyme because of the absence of the RecD translocating motor and since RecB translocates along the 3' ended strand in the 3' to 5' direction.

The advantage of the stopped-flow unwinding assay is that it is a continuous assay and thus many more time points can be obtained from a single experiment. As such, significantly more data from many more duplex lengths can be analyzed, yielding better estimates of the kinetic parameters. However, since the quenched-flow experiment yields a direct measure of the extent of DNA unwinding, we routinely perform and compare the results from both chemical quenched-flow and stopped-flow fluorescence studies. In this case, the kinetic parameters determined using both methods are in good agreement, although some slight differences in the parameters are observed (see Table 2).

RecBCD catalyzed unwinding of DNA duplexes with twin $(dT)_6$ ssDNA tails

We next compared RecBC and RecBCD unwinding directly. However, since the previous RecBCD experiments examined DNA unwinding from blunt DNA ends[41; 42], we needed to examine RecBCD unwinding of duplexes possessing the non-complementary twin dT_6 tails used in the RecBC studies. Figure 6A shows the time courses determined using the chemical quench-flow assay (the time courses determined using the stopped-flow assay are shown in Supplementary Figure 2A). The data in Figure 6A were analyzed by global NLLS analysis using the simple Scheme 1 (eq. 2) and the solid curves are time courses simulated using eq. 2 and the best fit parameters. Based on the poor quality of these fits, Scheme 1 is not sufficient to describe these time courses. Consistent with this conclusion, Figure 6B shows that a plot of the number of repeated rate limiting kinetic steps, *n*, versus duplex length, *L*, exhibits a positive y-intercept. The fact that the fitted value of *n* is not directly proportional to *L*, and that a positive y-intercept is observed suggests the presence of additional kinetic steps in the mechanism which are not directly associated with DNA unwinding[41; 44]. As a result, we re-analyzed these time courses using the more complicated Scheme 2 (eq. 4), in which *h* additional kinetic steps with rate constant k_C are included in the mechanism, although these steps are not repeated within the series of DNA unwinding cycles. Scheme 2 is the same kinetic scheme that was used previously to analyze RecBCD-catalyzed unwinding of a series of blunt-ended DNA duplexes[41; 42]. The time courses are well-described by Scheme 2, as shown in Figure 6C ($m = 3.3 \pm 1.3$ bp, $k_U = 240 \pm 56$ s^{-1}, $mk_U = 774 \pm 16$ bp/s, $h = 3.2 \pm 0.2$, $k_C = 45 \pm 2$, $k_{NP} = 1.1 \pm 0.3$ s^{-1}). Furthermore, after incorporating the additional k_C steps into the mechanism, the number of steps involved in unwinding, *n*, is found to be directly proportional to duplex length, *L*, while the number of additional steps, *h*, is independent of *L*, as shown in Figure 6D. A summary of the kinetic parameters obtained from the fits of the quenched-flow and fluorescence time courses to Scheme 2 is given in Table 2.

RecBCD-catalyzed unwinding of DNA possessing non-complementary 5'-$(dT)_{10}$ and 3'-$(dT)_6$ ssDNA tails

Previous equilibrium binding experiments have shown that RecBCD binds optimally to DNA duplex ends possessing non-complementary 5'-$(dT)_{10}$ and 3'-$(dT)_6$ ssDNA tails[37], hence we next examined RecBCD unwinding of DNA substrates possessing this DNA end structure under the same solution conditions used above. We first obtained time courses for five duplex lengths using the chemical quenched-flow unwinding assay. These time courses, shown in Figure 7A, also display lag kinetics and are biphasic. Interestingly, in contrast to the time courses obtained with the DNA substrates possessing twin $(dT)_6$ ssDNA tails, these time courses are well described by the simple *n*-step sequential kinetic mechanism of Scheme 1 as shown by the solid curves in Figure 7A ($m = 3.9 \pm 0.5$ bp, $k_U = 138 \pm 37$ s^{-1}, $mk_U = 538 \pm 24$ bp/s, $k_{NP} = 6.7 \pm 1.8$ s^{-1}). Furthermore, Figure 7B indicates that the number of steps involved in unwinding, *n*, is directly proportional to duplex length, *L*. The two to three additional steps, with rate constant k_C, that are part of Scheme 2 and required for RecBCD to initiate DNA unwinding from blunt-ends and duplexes with twin $(dT)_6$ tails, are not necessary to describe these time courses. This conclusion is also supported by time courses obtained for eight duplex lengths using the stopped-flow fluorescence assay (Supplementary Figure 3A and 3B). Table 2 provides a summary of the kinetic parameters obtained from these experiments. RecBCD has the same average kinetic step-size for unwinding (~ 4 bp) all three of the DNA molecules, independent of the end structure (blunt-end, twin $(dT)_6$, and 5'-$(dT)_{10}$, 3'-$(dT)_6$).

Discussion

In previous studies of the mechanism of RecBCD-catalyzed unwinding of DNA using single-turnover methods, Lucius et al.[40; 41; 42] found that the time course for RecBCD unwinding of blunt-ended DNA cannot be described by a simple sequential *n*-step kinetic model, such as that shown in Scheme 1. In fact, Scheme 2, which includes additional kinetic steps, was needed to describe the time courses for a range of duplex DNA lengths. The need to include these additional kinetic steps made it more difficult to estimate the DNA unwinding kinetic step-size for RecBCD, although a well-constrained kinetic step-size of (3.9 ± 0.5) bp was determined that is independent of ATP concentration and temperature[40]. The number (two to three) of these additional steps with rate constant, k_C, was found to be independent of DNA duplex length, hence, these steps do not appear to be part of the repeated cycles of DNA unwinding, and likely precede DNA unwinding[42].

The experiments described in our current study show that these additional steps are still required for RecBCD to initiate unwinding from a duplex end possessing non-complementary 5'-$(dT)_6$ and 3'-$(dT)_6$ ssDNA tails, yet they are not needed to describe the unwinding of DNA possessing a non-complementary 5'-$(dT)_{10}$ tail in the presence of a 3'-$(dT)_6$ ss-DNA tail. Interestingly, these additional steps are also not needed to describe the time course of RecBC catalyzed unwinding of DNA duplexes possessing non-complementary twin $(dT)_6$ ssDNA tails (Table 2). These results further support the conclusion that the additional k_C steps represent a real aspect of the mechanism for RecBCD initiation of DNA unwinding at a blunt-ended DNA. Furthermore, the less complex kinetic traces for RecBCD unwinding of duplex DNA possessing the non-complementary 5'-$(dT)_{10}$ and 3'-$(dT)_6$ ssDNA tails are well-described by the simple sequential *n*-step kinetic model (Scheme 1) and yield the same average kinetic step-size (~ 4 bp) as previously reported for RecBCD unwinding of blunt-ended DNA, thus supporting the previous analysis[40; 41; 42].

Functional significance of the additional k_C steps

The results from the current study, along with recent DNA binding[37] and structural studies[39] suggest a role for these additional kinetic steps with rate constant k_C. A crystal structure of RecBCD bound to a blunt-ended duplex shows 4 bp melted from the blunt end within the complex[39]; however, the four non-base paired nucleotides on the 5' ssDNA end do not contact any part of the RecD subunit. Equilibrium DNA binding studies[37] suggest that a 5'-ssDNA tail of at least ten nucleotides ($(dT)_{10}$) is needed to make full contact with the RecD subunit within the RecBCD-DNA complex. Computer modeling studies also suggest that extension of the 5'-ssDNA tail to 10 nucleotides is needed to contact the RecD subunit[46]. These findings suggest that the additional k_C steps that are required to describe RecBCD-catalyzed unwinding from a blunt-ended DNA duplex or a DNA duplex possessing twin $(dT)_6$ ssDNA tails reflect the process of initiating binding of the RecD subunit with the 5' ssDNA tail. This might involve pausing or molecular rearrangement steps that take place after the 5' ssDNA end becomes sufficient in length to reach RecD, thereby enabling this subunit to initiate DNA unwinding. In this scenario, upon ATP binding and hydrolysis, the RecB motor in the RecBCD-DNA complex, acting on the 3' ssDNA strand would begin to unwind the duplex and translocate along the DNA until it creates a long enough 5' ssDNA tail, at least ten nucleotides, so that RecD can interact with the 5' ssDNA strand and initiate translocation. Studies of the $RecB^{K29Q}CD$ protein, where the RecB motor is inactivated via a mutation in the ATP binding site[47] showed that a 4 nucleotide 5' ssDNA tail on the DNA end is required for DNA unwinding. This observation is consistent with our results since upon melting of the 6 base pairs at the duplex DNA end, this would yield a 10 nucleotide long 5'-ss-DNA tail, which would allow interaction of RecD.

Interestingly, although the additional k_C steps are not needed to describe RecBCD unwinding of duplex DNA possessing non-complementary 5-$(dT)_{10}$ and 3'-$(dT)_6$ ssDNA tails, the macroscopic rate of DNA unwinding that we estimate is slightly slower (538 ± 24 bp s^{-1}) than for RecBCD unwinding of a blunt-ended DNA (790 ± 23 bp s^{-1}) or a duplex DNA possessing non-complementary twin $(dT)_6$ tails (774 ± 16 bp s^{-1}). Currently, we cannot explain this slower observed rate of DNA unwinding. However, it has recently been shown that the rate of RecBCD unwinding becomes slower after RecBCD interacts with a “chi” sequence in the unwound ssDNA due to a switching of the lead motor from RecD to RecB[23]. In light of this, it is possible that when RecBCD initiates unwinding from a blunt-ended DNA or a duplex end possessing non-complementary 3'-$(dT)_6$ and 5'-$(dT)_6$ tails, it starts in a “pre-chi” state with a faster rate. However, when RecBCD initiates unwinding from a duplex end possessing an extended 5' ssDNA tail of ten nucleotides, it may initiate unwinding as if it were in a “post-chi” state. Further experiments will be needed to test this hypothesis.

We note that there is a potential ambiguity in the analyses of the experiments reported here, specifically with regard to the actual length of duplex DNA that should be considered unwound by RecBCD or RecBC during its ATP-dependent unwinding (helicase) reaction. We find that the kinetic parameters determined for RecBCD unwinding of a series of blunt-ended DNA duplexes varying in length, *L* (bp), are identical within experimental error to the kinetic parameters determined for RecBCD unwinding of a series of DNA duplexes possessing non-complementary 5'- and 3'-$(dT)_6$ tails. However, when RecBCD forms an initiation complex with a blunt duplex DNA end, the enzyme can “melt-out” 5–6 bp in a Mg^{2+} or Ca^{2+}-dependent reaction[37; 38; 39], hence the effective duplex length with pre-bound RecBCD is potentially ~ 5–6 bp shorter than the actual length of the duplex region. Yet, when RecBCD binds to a DNA end possessing non-complementary twin $(dT)_6$ ssDNA tails or 5-$(dT)_{10}$ and 3'-$(dT)_6$ ssDNA tails, no additional bp melting presumably occurs[37]. This becomes an issue when we relate the number of kinetic steps, *n*, determined from the NLLS analysis to the length of the duplex DNA that is unwound, which in turn would potentially

affect the estimation of the kinetic step-size, *m*. In an attempt to assess the effects of this ambiguity, we reanalyzed the time courses for RecBCD-catalyzed unwinding of blunt-ended DNA in two ways. We assumed that each DNA duplex length is actually (*L*-6) bp rather than *L* bp when RecBCD is initially bound to the blunt-ended DNA, but before unwinding is initiated. We then compared the plots of *n vs* (*L*-6) and *n vs L* for the blunt-ended duplexes with the plot of *n* vs *L* for RecBCD unwinding of the twin $(dT)_6$ tailed DNA substrate. We find that the kinetic parameters determined from these three analyses are identical within our experimental uncertainty; hence this potential ambiguity has no influence on the kinetic parameters that we report here. On the other hand, even though RecBCD melts out 5–6 bp upon binding to a blunt DNA end, the enzyme may still need to proceed through the same number, *n*, of repeated rate-limiting steps to fully unwind a blunt-ended DNA of duplex length, *L*, or a DNA with duplex length (*L-6*) bp that possesses non-complementary twin $(dT)_6$ tails. This could result if the *n* repeated rate-limiting kinetic steps are not associated with the actual DNA unwinding process, which may be much faster, but rather with a slower process (e.g., a protein conformational change) that is repeated every ~4 bp (on average) during the unwinding cycle. Hence, even if 5–6 bp of a duplex end are pre-melted, the "kinetic step" may not be complete until it proceeds through the rate-limiting step and thus the total number of rate-limiting steps needed to fully unwind the DNA could be unchanged.

RecBC and RecBCD display the same average kinetic step-size for DNA unwinding

We have shown that RecBC initiates DNA unwinding poorly from a blunt DNA end and that its ability to initiate unwinding is greatly enhanced when RecBC is pre-bound to a duplex possessing non-complementary twin dT_6 ssDNA tails. We have recently shown that RecBC appears able to melt out at least 4 bp upon binding to a blunt DNA duplex end in a Mg^{2+}-dependent, but ATP-independent reaction[48], similar to the reaction demonstrated for RecBCD[38]. However, the kinetic results reported here suggest that the complex formed by RecBC upon binding to a blunt DNA end must differ in some important functional manner from the RecBCD complex. Yet, once initiated, RecBC unwinds DNA with an average kinetic step-size of ~ 4 bp, which is the same as the average kinetic step-size for RecBCD unwinding. RecBC unwinding studies performed as a function ATP concentration (C. Wu and T. M. Lohman, unpublished data) indicate that this average kinetic step-size is also independent of ATP concentration, as observed previously for RecBCD[40]. These data suggest that the same rate limiting kinetic process is repeated every ~4 bp on average during DNA unwinding by both RecBCD and RecBC, although the rate of this process is slower for RecBC.

It is not clear how the kinetic step size measured in our single turnover ensemble studies may relate to a mechanical step size, as measured in a single molecule experiment. However, it is worth noting that these should only be the same if the process that limits the rate of DNA unwinding is the same as the process that limits the rate of the mechanical step. For example, Bianco and Kowalczykowski[45] have proposed a "quantum inch worm model" for RecBC unwinding and translocation based on the observation that RecBC is able to bypass flexible ss-DNA gaps in duplex DNA as large as ~23 nucleotides. In this model, the enzyme is viewed as having two DNA binding sites such that DNA unwinding occurs in a series of small steps of a few base pairs, whereas larger translocation steps of ~23 bp can also occur. In this model, the unwinding step-size could be smaller than the translocation step-size. Based on the experiments reported here we observe a smaller (~4 bp) kinetic step size for RecBC unwinding. However, if translocation and unwinding occur with different step sizes, the relative rates of the steps limiting unwinding vs. translocation would determine which step is observed in a measurement of a kinetic step size. Previous single molecule studies of RecBCD unwinding[49] were unable to resolve individual steps, although those experiments placed an upper limit for the step size of a few base pairs.

Materials and Methods

Buffers and Reagents

Buffers were prepared with reagent grade chemicals and double-distilled water that was deionized further using a Milli-Q purification system (Millipore Corp., Bedford, MA). All buffers and reagents were filtered using 0.2 micron filters after preparation. RecBCD storage buffer is Buffer C: 20 mM KP_i (pH 6.8 at 25°C), 0.1 mM 2-mercaptoethanol (2-ME), 0.1 mM EDTA, 10% (v/v) glycerol. DNA unwinding reaction buffer is Buffer M: 20 mM Mops-KOH (pH 7.0 at 25°C), 30 mM NaCl, 10 mM $MgCl_2$, 1 mM 2-ME, 5% (v/v) glycerol.

Heparin stock solutions were prepared by dissolving heparin sodium salt (Sigma, St. Louis, MO, Lot No.114K1328) in Buffer M and dialyzing further against Buffer M using 3500 molecular weight cut-off (MWCO) dialysis tubing. Heparin stock concentrations were determined by titration with Azure A as described[50] and stored at 4°C until use.

ATP stock solutions were prepared by dissolving adenosine 5'-triphosphate sodium salt (Sigma, St. Louis, MO, Lot No.016K7008) in water and adjusting the pH to 7.0 with NaOH. Stock aliquots were stored at −20°C until use and stock concentrations were determined spectrophotometrically using an extinction coefficient of $\varepsilon_{260} = 1.5\times10^4\ M^{-1}cm^{-1}$[51].

Proteins

E. coli RecB and RecC were purified and stored in Buffer C at −80°C as described[41; 42]. The RecBC enzyme was reconstituted by mixing equimolar RecB and RecC on ice. RecBC was dialyzed against Buffer M at 4°C before use, and its concentration was determined spectrophotometrically using an extinction coefficient of $\varepsilon_{280} = 3.9\times10^5\ M^{-1}cm^{-1}$[37]. We have examined compared our RecBC preparation with RecBC that was purified from *E. coli* directly as the heterodimer (kindly provided by A. Taylor and G. Smith (Fred Hutchinson Cancer Center, Seattle, WA)) and observed no differences between the two preparations with respect to DNA binding[37] and single turnover DNA unwinding. On the other hand, in multiple turnover experiments, Bianco and Kowalczykowski[45] observe that ~ 65% of a blunt-ended DNA substrate is unwound after two minutes. For comparison, we also performed multiple turnover unwinding experiments with a 24 base pair blunt ended DNA substrate (Substrate I without the non-complementary $(dT)_n$ tails) under the same solution conditions used in that study[45] and observed similar results (~56% unwinding after two minutes).

E. coli RecBCD was purified as a heterotrimer and stored in Buffer C at −80°C as described[36; 41; 52; 53]. RecBCD was dialyzed against Buffer M at 4°C before use, and its concentration was determined spectrophotometrically using an extinction coefficient of $\varepsilon_{280} = 4.5\times10^5\ M^{-1}cm^{-1}$ [36; 41; 52; 53]. Dialyzed RecBCD and RecBC was used immediately (within a day) since a loss of activity (5–15%) occurred after five days at 4°C in Buffer M[36; 37; 41; 52; 53].

Bovine serum albumin (BSA) was purchased from Roche (Indianapolis, IN) and dialyzed against Buffer M at 4°C. Dialyzed BSA stock was stored at 4°C until use and stock concentration was determined spectrophotometrically using an extinction coefficient of $\varepsilon_{280} = 4.3\times10^4\ M^{-1}cm^{-1}$ [37; 54]

Oligodeoxynucleotides

Oligodeoxynucleotides were synthesized using an ABI model 391 synthesizer (Applied Biosystems, Foster City, CA) as described[55]. Unlabeled DNA was purified using polyacrylamide gel electrophoresis under denaturing conditions followed by gel

electroelution while Cy3 and Cy5 labeled DNA was further purified by reverse phase HPLC using an XTerra MS C18 column (Waters, Milford, MA)[55]. The concentrations of each stock of DNA strands were determined by digesting each strand with phosphodiesterase I (Worthington, Lakewood, NJ) in 100 mM Tris-HCl (pH 9.2 at 25°C), 3 mM $MgCl_2$, and analyzing the resulting mixture of mononucleotides spectrophotometrically using the following extinction coefficients[51]: $\varepsilon_{260,AMP}$ = 15,340 $M^{-1}cm^{-1}$, $\varepsilon_{260,CMP}$ = 7,600 $M^{-1}cm^{-1}$, $\varepsilon_{260,GMP}$ = 12,160 $M^{-1}cm^{-1}$, $\varepsilon_{260,TMP}$ = 8,700 $M^{-1}cm^{-1}$, $\varepsilon_{260,Cy63}$ = 5,000 $M^{-1}cm^{-1}$, $\varepsilon_{260,Cy5}$ = 10,000 $M^{-1}cm^{-1}$.

DNA substrate design

The DNA substrates used for DNA unwinding studies were composed of three DNA strands which form a hairpin structure when annealed together with the exception of two nicks as shown in Figure 1[36; 41; 42]. For chemical quenched-flow experiments, strand A was radiolabeled on its 5' end as depicted in Figure 1A with ^{32}P using T4 polynucleotide kinase (USB, Cleveland, OH) and $\gamma^{32}P$-ATP (Perkin Elmer, Waltham, MA) as described[55]. The radiolabeled strand A was mixed with an equal molar ratio of strand B and 25% excess of the bottom strand. The resulting DNA stock solution was heated to 94°C for five minutes followed by slow cooling to 25°C to allow annealing. For stopped-flow unwinding experiments, strand A was fluorescently labeled with a Cy3 donor while strand B was labeled with a Cy5 acceptor as depicted in Figure 1B. These two fluorescently labeled DNA strands were mixed and annealed to the bottom strand as described above.

Rapid chemical quenched-flow DNA unwinding kinetics

DNA unwinding experiments were performed at 25°C using a quenched-flow apparatus (KinTek RQF-3, University Park, PA) as described[41]. RecBCD or RecBC (20 nM) was pre-incubated with ^{32}P labeled DNA substrate (2 nM) and BSA (6 μM) on ice for 20 minutes in Buffer M and this mixture was then loaded into one loop of the quenched-flow apparatus. Equilibrium binding experiments indicate that all unwinding substrates were saturated under these solution conditions and at these protein and DNA concentrations[37]. A solution containing ATP (10 mM) and heparin trap (15 mg/ml) in Buffer M was loaded into the other loop. After equilibration at 25°C for five minutes, DNA unwinding was initiated by rapidly mixing these solutions together (1:1) and quenching the reaction after a predefined time interval (Δt) by mixing with 0.4 M EDTA, 10% (v/v) glycerol; the zero time-point was determined by performing a “mock reaction” (without ATP). Quenched reactions collected at each time-point were kept on ice until all samples were collected, and the unwound ssDNA was separated from the native duplex DNA using non-denaturing polyacrylamide (10% (w/v)) gel electrophoresis. The gel was exposed to a phosphor screen (Molecular Dynamics, Sunnyvale, CA) for one hour after which the screen was scanned using a Storm 840 phosphorimager (Molecular Dynamics, Sunnyvale, CA). The radioactivity of each band was quantified using the ImageQuant software (Molecular Dynamics, Sunnyvale, CA) and the fraction of DNA molecules unwound at each time-point, $f_{ss}(t)$, was calculated using Equation 1[41]:

$$f_{ss}(t) = \frac{\frac{C_S(t)}{C_S(t)+C_D(t)} - \frac{C_{S,0}}{C_{S,0}+C_{D,0}}}{1 - \frac{C_{S,0}}{C_{S,0}+C_{D,0}}} \quad (1)$$

where $C_S(t)$ and $C_D(t)$ reflects the radioactive counts for the unwound ssDNA and the native duplex DNA, respectively at time t, while $C_{S,0}$ and $C_{D,0}$ represent the corresponding quantities at time zero. Unwinding time courses were collected as a function of duplex

length (L = 24, 30, 40, 48, and 60 bp) and the averages of three independent unwinding time courses for each duplex length were subjected to global NLLS analysis.

Stopped-flow fluorescence unwinding kinetics

Fluorescence DNA unwinding experiments were performed at 25°C using a stopped-flow apparatus (SX.18MV, Applied Photophysics Ltd, Leatherhead, UK) as described[40; 42]. RecBC or RecBCD (200 nM) was pre-incubated with each Cy3-Cy5 labeled DNA substrate (40 nM) and BSA (6 μM) on ice for 20 minutes in Buffer M. Equilibrium binding experiments indicate that all unwinding substrates were saturated under these solution conditions and at these protein and DNA concentrations[37]. This mixture was then loaded into one syringe of the stopped-flow apparatus, and a solution containing ATP (10 mM) and heparin (15 mg/ml) in Buffer M was loaded into the other syringe of the device. Both solutions were equilibrated to 25°C for five minutes after which DNA unwinding was initiated by rapid mixing of the two solutions (1:1). The Cy3 fluorophore was excited at 515 nm and its emission was monitored at 570 nm with an interference filter (Oriel Corp., Stradford, CT); Cy5 emission was monitored simultaneously at all wavelengths > 665 nm using a long pass filter (Oriel Corp., Stradford, CT). 10 individual Cy3 FRET time courses were collected and averaged, and unwinding experiments were performed as a function of duplex length (L = 24, 29, 37, 40, 43, 48, 53, and 60 bp). The results from three independent measurements were averaged and subjected to global NLLS analysis. Since all Cy3 FRET time courses exhibit a lag phase before fluorescence enhancement, this initial signal was assumed to represent 100% duplex DNA and thus reflect zero DNA unwinding. Hence, the first ten data points from each time-course were averaged and subtracted from all data points, thereby constraining each time-course to start at zero[42].

Analysis of DNA Unwinding Kinetics

Global NLLS analysis of DNA unwinding kinetics was performed as described[41; 42; 44] using Conlin 56 (kindly provided by Dr. Jeremy Williams and modified by Dr. Chris Fischer) and IMSL C Numerical Libraries (Visual Numeric Incorporated, Houston, TX). The uncertainties reported reflect 68% confidence interval limits determined from a 50 cycle Monte Carlo analysis as described[41]. Entire time courses with data collected out to 10 seconds were used in the analysis although only data out to 0.4 seconds was plotted here for clarity. Fitting of the time courses to a particular kinetic scheme was performed by obtaining the time-dependent formation of ssDNA, $f_{ss}(t)$, as the inverse Laplace transform of $F_{ss}(s)$ using numerical methods as described[41; 44]. For Scheme 1, $f_{ss}(t)$ is given by Equation 2:

$$\begin{aligned} f_{ss}(t) &= A_T \mathrm{L}^{-1} F_{ss}(s) \\ &= A_T \mathrm{L}^{-1} \left(\frac{k_U^n (k_{NP} + sx)}{s(k_{NP} + s)(k_U + s)^n} \right) \end{aligned} \tag{2}$$

where $F_{ss}(s)$ is the Laplace transform of $f_{ss}(t)$, L^{-1} is the inverse Laplace transform operator with s as the Laplace variable, A_T is the total amplitude for a given duplex length L, n is the number of unwinding steps with k_U being the rate constant in between two successive unwinding steps, k_{NP} is the rate constant for the isomerization reaction from non-productive, $(RD)_{NP}$, to productive, $(RD)_L$, RecBC(D)-DNA complexes, and x is the fraction of productively bound RecBC(D)-DNA complexes defined by Equation 3:

$$x = \frac{(RD)_L}{(RD)_L + (RD)_{NP}} \tag{3}$$

$f_{ss}(t)$ for Scheme 2 is given by Equation 4 in which h additional kinetic steps with rate constant k_C that are not directly associated with DNA unwinding have been included in the mechanism:

$$\begin{aligned} f_{ss}(t) &= A_T \mathrm{L}^{-1} F_{ss}(s) \\ &= A_T \mathrm{L}^{-1} \left(\frac{k_C^h k_U^n (k_{NP} + sx)}{s(k_C + s)^h (k_{NP} + s)(k_U + s)^n} \right) \end{aligned} \quad (4)$$

In Figures 4B, 5B, 6B, 7B, and 8B, A_T, n, h (where appropriate), and x were allowed to float for each duplex length while k_C (where appropriate), k_U, and k_{NP} were constrained to be global parameters. In Figures 4A, 5A, 6A, 7A, and 8A, n in Equation 2 and Equation 4 was replaced with L/m, where L is duplex length in base pairs and m is the average unwinding kinetic step-size. In this analysis, A_T and x (as well as h where appropriate) were floated for each time-course at every duplex length while k_U, k_{NP}, and m (as well as k_C where appropriate) were constrained to be global parameters.

Supplementary Material

Refer to Web version on PubMed Central for supplementary material.

Acknowledgments

We thank Thang Ho for synthesis and purification of all DNA substrates, Drs. Gerald Smith and Doug Julin for providing plasmids and cell lines, and Drs. Aaron Lucius, Anita Niedziela-Majka, and Jason Wong for valuable discussions. This work was supported in part by NIH grant GM045948.

References

1. Lohman TM, Bjornson KP. Mechanisms of Helicase-Catalyzed DNA Unwinding. Ann.Rev.Biochem. 1996; 65:169–214. [PubMed: 8811178]
2. Lohman, TM.; Hsieh, J.; Maluf, NK.; Cheng, W.; Lucius, AL.; Fischer, CJ.; Brendza, KM.; Korolev, S.; Waksman, A. DNA Helicases, Motors that Move Along Nucleic Acids: Lessons from the SF1 Helicase Superfamily. In: Tamanoi, F.; Hackney, DD., editors. The Enzymes. Academic Press; NY: 2003. p. XXIII
3. Matson SW, Bean DW, George JW. DNA helicases: enzymes with essential roles in all aspects of DNA metabolism. Bioessays. 1994; 16:13–22. [PubMed: 8141804]
4. Patel SS, Donmez I. Mechanisms of Helicases. J. Biol. Chem. 2006; 281:18265–18268. [PubMed: 16670085]
5. Patel SS, Picha KM. Structure and function of hexameric helicases. Annu Rev Biochem. 2000; 69:651–97. [PubMed: 10966472]
6. Delagoutte E, von Hippel PH. Helicase mechanisms and the coupling of helicases within macromolecular machines. Part I: Structures and properties of isolated helicases. Q Rev Biophys. 2002; 35:431–78. [PubMed: 12621862]
7. Singleton MR, Dillingham MS, Wigley DB. Structure and Mechanism of Helicases and Nucleic Acid Translocases. Annu Rev Biochem. 2007; 76:23–50. [PubMed: 17506634]
8. Flores MJ, Sanchez N, Michel B. A fork-clearing role for UvrD. Mol Microbiol. 2005; 57:1664–75. [PubMed: 16135232]
9. Jankowsky E, Gross CH, Shuman S, Pyle AM. Active disruption of an RNA-protein interaction by a DExH/D RNA helicase. Science. 2001; 291:121–5. [PubMed: 11141562]
10. Veaute X, Delmas S, Selva M, Jeusset J, Le Cam E, Matic I, Fabre F, Petit MA. UvrD helicase, unlike Rep helicase, dismantles RecA nucleoprotein filaments in *Escherichia coli*. EMBO J. 2005; 24:180–9. [PubMed: 15565170]

11. Eggleston AK, O'Neill TO, Bradbury EM, Kowalczykowski SC. Unwinding of Nucleosomal DNA by a DNA Helicase. J.Biol.Chem. 1995; 270:2024–2031. [PubMed: 7836428]
12. Byrd AK, Raney KD. Displacement of a DNA binding protein by Dda helicase. Nucl. Acids Res. 2006; 34:3020–9. [PubMed: 16738140]
13. German J, Sanz MM, Ciocci S, Ye TZ, Ellis NA. Syndrome-causing mutations of the BLM gene in persons in the Bloom's Syndrome Registry. Hum Mutat. 2007; 28:743–53. [PubMed: 17407155]
14. Ellis NA, Groden J, Ye T-Z, Straughen J, Lennon DJ, Ciocci S, Proytcheva M, German J. The Bloom's syndrome gene product is homologous to RecQ helicases. Cell. 1995; 83:655–666. [PubMed: 7585968]
15. Hickson ID, Davies SL, Li JL, Levitt NC, Mohaghegh P, North PS, Wu L. Role of the Bloom's syndrome helicase in maintenance of genome stability. Biochem Soc Trans. 2001; 29:201–4. [PubMed: 11356154]
16. Hickson ID. RecQ helicases: caretakers of the genome. Nat Rev Cancer. 2003; 3:169–78. [PubMed: 12612652]
17. Finch PW, Storey A, Brown K, Hickson ID, Emmerson PT. Complete nucleotide sequence of *recD*, the structural gene for the α subunit of Exonuclease V of *Escherichia coli*. Nucleic Acids Research. 1986; 14:8583–8594. [PubMed: 3537961]
18. Finch PW, Storey A, Chapman KE, Brown K, Hickson ID, Emmerson PT. Complete nucleotide sequence of the *Escherichia coli recB* gene. Nucleic Acids Research. 1986; 14:8573–8582. [PubMed: 3537960]
19. Finch PW, Wilson RE, Brown K, Hickson ID, Tomkinson AE, Emmerson PT. Complete nucleotide sequence of the Escherichia coli recC gene and of the thyA-recC intergenic region. Nucleic Acids Res. 1986; 14:4437–51. [PubMed: 3520484]
20. Anderson DG, Kowalczykowski SC. The Translocating RecBCD Enzyme Stimulates Recombination by Directing RecA Protein onto ssDNA in a χ-regulated Manner. Cell. 1997; 90:77–86. [PubMed: 9230304]
21. Kowalczykowski SC, Dixon DA, Eggleston AK, Lauder SD, Rehrauer WM. Biochemistry of homologous recombination in *Escherichia coli*. Microbiological Reviews. 1994; 58:401–465. [PubMed: 7968921]
22. Smith, GR. RecBCD Enzyme. In: Eckstein, F.; Lilley, DMJ., editors. Nucleic Acids and Molecular Biology. Springer Verlag; Berlin: 1990. p. 78-98.
23. Spies M, Amitani I, Baskin RJ, Kowalczykowski SC. RecBCD Enzyme Switches Lead Motor Subunits in Response to chi Recognition. Cell. 2007; 131:694–705. [PubMed: 18022364]
24. Yu M, Souaya J, Julin DA. The 30-kDa C-terminal domain of the RecB protein is critical for the nuclease activity, but not the helicase activity, of the RecBCD enzyme from *Escherichia coli*. Proc.Natl.Acad.Sci.,U.S.A. 1998; 95:981–986. [PubMed: 9448271]
25. Yu M, Souaya J, Julin DA. Identification of the Nuclease Active Site in the Multifunctional RecBCD Enzyme by Creation of a Chimeric Enzyme. J.Mol.Biol. 1998; 283:797–808. [PubMed: 9790841]
26. Bianco PR, Brewer LR, Corzett M, Balhorn R, Yeh Y, Kowalczykowski SC, Baskin RJ. Processive translocation and DNA unwinding by individual RecBCD enzyme molecules. Nature. 2001; 409:374–378. [PubMed: 11201750]
27. Handa N, Bianco PR, Baskin RJ, Kowalczykowski SC. Direct visualization of RecBCD movement reveals cotranslocation of the RecD motor after chi recognition. Mol Cell. 2005; 17:745–50. [PubMed: 15749023]
28. Spies M, Bianco PR, Dillingham MS, Handa N, Baskin RJ, Kowalczykowski SC. A molecular throttle: the recombination hotspot chi controls DNA translocation by the RecBCD helicase. Cell. 2003; 114:647–54. [PubMed: 13678587]
29. Arnold DA, Kowalczykowski SC. Facilitated loading of RecA protein is essential to recombination by RecBCD enzyme. J Biol Chem. 2000; 275:12261–5. [PubMed: 10766864]
30. Gorbalenya AE, Koonin EV. Helicases: amino acid sequence comparisons and structure-function relationships. Curr.Op.Struct.Biol. 1993; 3:419–429.
31. Dillingham MS, Spies M, Kowalczykowski SC. RecBCD enzyme is a bipolar helicase. Nature. 2003; 423:893–897. [PubMed: 12815438]

32. Taylor AF, Smith GR. RecBCD enzyme is a DNA helicase with fast and slow motors of opposite polarity. Nature. 2003; 423:889–893. [PubMed: 12815437]
33. Roman LJ, Eggleston AK, Kowalczykowski SC. Processivity of the DNA helicase activity of Escherichia coli recBCD enzyme. J Biol Chem. 1992; 267:4207–14. [PubMed: 1310990]
34. Roman LJ, Kowalczykowski SC. Characterization of the helicase activity of the Escherichia coli RecBCD enzyme using a novel helicase assay. Biochemistry. 1989; 28:2863–73. [PubMed: 2545238]
35. Masterson C, Boehmer PE, McDonald F, Chaudhuri S, Hickson ID, Emmerson PT. Reconstitution of the activities of the RecBCD holoenzyme of Escherichia coli from the purified subunits. J Biol Chem. 1992; 267:13564–72. [PubMed: 1618858]
36. Taylor AF, Smith GR. Monomeric RecBCD Enzyme Binds and Unwinds DNA. J.Biol.Chem. 1995; 270:24451–24458. [PubMed: 7592660]
37. Wong CJ, Lucius AL, Lohman TM. Energetics of DNA end binding by *E.coli* RecBC and RecBCD helicases indicate loop formation in the 3'-single-stranded DNA tail. J. Mol. Biol. 2005; 352:765–82. [PubMed: 16126227]
38. Farah JA, Smith GR. The RecBCD Enzyme Initiation Complex for DNA Unwinding: Enzyme Positioning and DNA Opening. J.Mol.Biol. 1997; 272:699–715. [PubMed: 9368652]
39. Singleton MR, Dillingham MS, Gaudier M, Kowalczykowski SC, Wigley DB. Crystal structure of RecBCD enzyme reveals a machine for processing DNA breaks. Nature. 2004; 432:187–93. [PubMed: 15538360]
40. Lucius AL, Lohman TM. Effects of temperature and ATP on the kinetic mechanism and kinetic step-size for *E.coli* RecBCD helicase-catalyzed DNA unwinding. J. Mol. Biol. 2004; 339:751–71. [PubMed: 15165848]
41. Lucius AL, Vindigni A, Gregorian R, Ali JA, Taylor AF, Smith GR, Lohman TM. DNA Unwinding Step-size of *E. coli* RecBCD Helicase Determined from Single Turnover Chemical Quenched-flow Kinetic Studies. J. Mol. Biol. 2002; 324:409–428. [PubMed: 12445778]
42. Lucius AL, Jason Wong C, Lohman TM. Fluorescence stopped-flow studies of single turnover kinetics of *E.coli* RecBCD helicase-catalyzed DNA unwinding. J. Mol. Biol. 2004; 339:731–50. [PubMed: 15165847]
43. Ali JA, Lohman TM. Kinetic Measurement of the Step-size of DNA Unwinding by *Escherichia coli* UvrD Helicase. Science. 1997; 275:377–380. [PubMed: 8994032]
44. Lucius AL, Maluf NK, Fischer CJ, Lohman TM. General methods for analysis of sequential “n-step” kinetic mechanisms: application to single turnover kinetics of helicase-catalyzed DNA unwinding. Biophys J. 2003; 85:2224–39. [PubMed: 14507688]
45. Bianco PR, Kowalczykowski SC. Translocation step size and mechanism of the RecBC DNA helicase. Nature. 2000; 405:368–372. [PubMed: 10830968]
46. Wong CJ, Rice RL, Baker NA, Ju T, Lohman TM. Probing 3'-ssDNA Loop Formation in *E. coli* RecBCD/RecBC-DNA Complexes Using Non-natural DNA: A Model for “Chi” Recognition Complexes. J. Mol. Biol. 2006; 362:26–43. [PubMed: 16901504]
47. Dillingham MS, Webb MR, Kowalczykowski SC. Bipolar DNA translocation contributes to highly processive DNA unwinding by RecBCD enzyme. J Biol Chem. 2005; 280:37069–77. [PubMed: 16041061]
48. Wong CJ, Lohman TM. Kinetic Control of Mg^{2+}-dependent Melting of Duplex DNA Ends by *E. coli* RecBC. J. Molecular Biology. 2008 in press.
49. Perkins TT, Li HW, Dalal RV, Gelles J, Block SM. Forward and reverse motion of single RecBCD molecules on DNA. Biophys J. 2004; 86:1640–8. [PubMed: 14990491]
50. Mascotti DP, Lohman TM. Thermodynamics of charged oligopeptide-heparin interactions. Biochemistry. 1995; 34:2908–15. [PubMed: 7893705]
51. Gray DM, Hung SH, Johnson KH. Absorption and Circular Dichroism Spectroscopy of Nucleic Acid Duplexes and Triplexes. Methods in Enzymology. 1995; 246:19–34. [PubMed: 7538624]
52. Amundsen SK, Taylor AF, Chaudhury AM, Smith GR. recD: the gene for an essential third subunit of exonuclease V. Proc.Natl.Acad.Sci.USA. 1986; 83:5558–5562. [PubMed: 3526335]
53. Taylor AF, Smith GR. Substrate specificity of the DNA unwinding activity of the recBC enzyme of *Escherichia coli*. J.Mol.Biol. 1985; 185:431–443. [PubMed: 2997450]

54. Lohman TM, Chao K, Green JM, Sage S, Runyon G. Large-scale purification and characterization of the *Escherichia coli rep* gene product. J.Biol.Chem. 1989; 264:10139–10147. [PubMed: 2524489]

55. Wong I, Chao KL, Bujalowski W, Lohman TM. DNA-induced dimerization of the Escherichia coli rep helicase. Allosteric effects of single-stranded and duplex DNA. J Biol Chem. 1992; 267:7596–-610. [PubMed: 1313807]

56. Williams DJ, Hall KB. Monte Carlo Applications to Thermal and Chemical Denaturation Experiments of Nucleic Acids and Proteins. Methods in Enzymology. 2000; 321:330–352. [PubMed: 10909065]

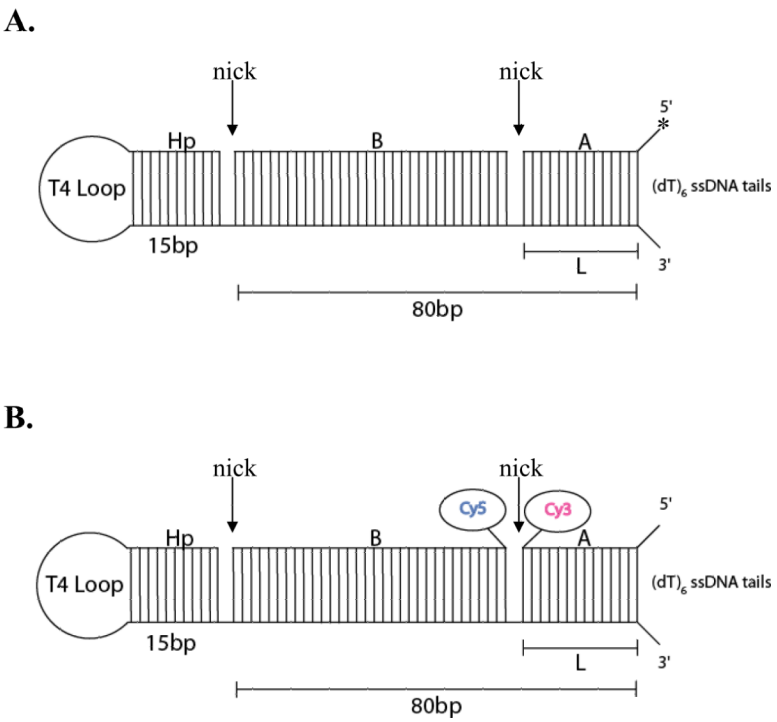

Figure 1.

Schematic representation of DNA substrates used in unwinding studies. Each DNA substrate is composed of three oligodeoxynucleotide strands, a constant bottom strand containing a hairpin (Hp), and two top strands—A and B. These three DNA strands anneal to form a hairpin duplex containing two nicks. DNA substrates of different duplex lengths, *L*, are formed by varying the lengths of strands A and B while keeping their combined length constant. Because most substrates used in our unwinding studies possess non-complementary ssDNA tails, *L* refers to the length of strand A that is base paired with the bottom strand and therefore must be unwound before DNA unwinding can be detected. (**A**). DNA substrates used in chemical quenched-flow unwinding experiments. Strand A is radiolabeled with ^{32}P at its 5' end (denoted by an asterisk) and the release of this strand is used to monitor DNA unwinding. (**B**). DNA substrates used in stopped-flow fluorescence measurements. A Cy3 and Cy5 FRET pair is positioned across a nick as depicted and changes in FRET signal are used to monitor DNA unwinding.

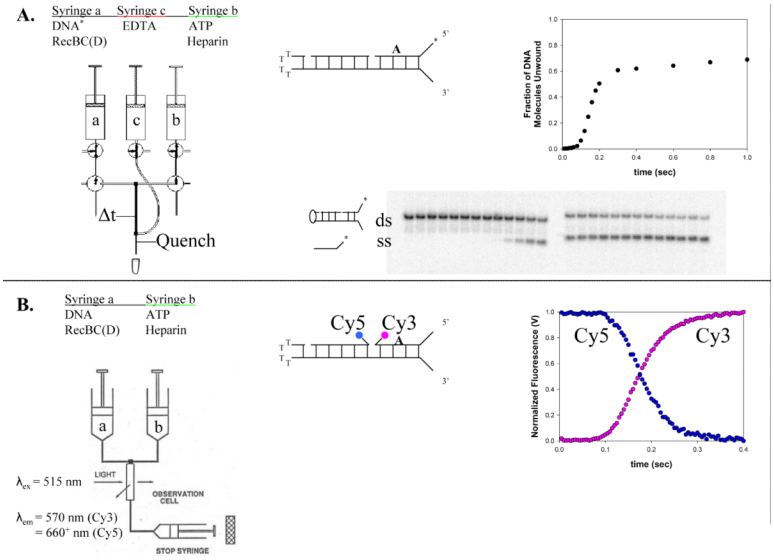

Figure 2.

Design of “all or none” chemical quenched-flow and stopped-flow fluorescence experiments to study single turnover kinetics of DNA unwinding. (**A**)-Quenched-flow assay. DNA substrates (radiolabeled with ^{32}P on the 5' end of strand “A”) are incubated with excess RecBCD or RecBC helicase in one syringe. DNA unwinding is initiated by rapid mixing with ATP and heparin. The unwinding reaction is quenched after a time interval (Δt) by rapid mixing with EDTA, and the ssDNA product produced after each time interval is separated from the native duplex DNA using non-denaturing polyacrylamide gel electrophoresis and analyzed quantitatively after exposure to a phosphorimager (see Materials and Methods for details). (**B**). Stopped-flow assay. A DNA substrate labeled with donor (Cy3) and acceptor (Cy5) fluorophores as indicated is incubated with excess RecBCD or RecBC in one syringe and DNA unwinding is initiated by rapid mixing with ATP and heparin. When in Cy3 and Cy5 fluorophores are in close proximity, Cy3 fluorescence is decreased and Cy5 fluorescence is increased due to fluorescence energy transfer (FRET). DNA unwinding is monitored in real time by the concomitant increase in Cy3 fluorescence and decrease in Cy5 fluorescence accompanying DNA unwinding and release of strand “A”. Cy3 fluorescence is excited at 515 nm and Cy3 fluorescence emission is monitored at 570 nm using an interference filter, while Cy5 fluorescence emission is monitored simultaneously at wavelengths above 665 nm using a long pass filter.

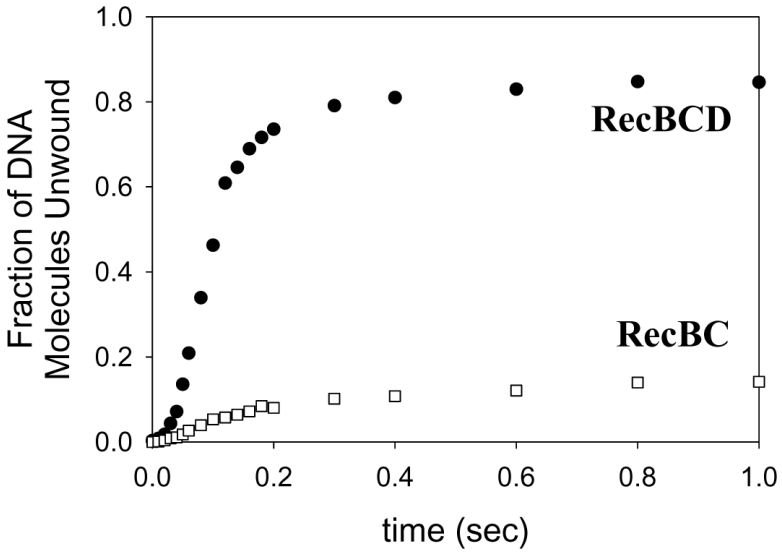

Figure 3.

Comparison of the kinetics of DNA unwinding of a 24 bp blunt-ended DNA substrate (Substrate I without non-complementary dT tails) by RecBCD and RecBC. Single turnover time courses, obtained using the quenched-flow assay, show that RecBCD (J) initiates unwinding from a blunt DNA end with much higher efficiency than does RecBC (G).

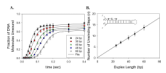

Figure 4.

Single-turnover kinetics of RecBC catalyzed unwinding of DNA duplexes possessing non-complementary 5'-$(dT)_6$ and 3'-$(dT)_6$ ssDNA tails. **(A).** Time courses as a function of duplex length (*L* = 24 bp, (J); *L* = 30 bp, (B); *L* = 40 bp, (H); *L* = 48 bp, (F); *L* = 60 bp, (S)) obtained using the quenched-flow assay. Data points correspond to the average of three independent measurements and the error bars indicate the standard deviation of the data. Smooth curves are simulated time courses based on the global NLLS best fits to Scheme 1, with: mk_{obs} = 396 ± 15 bp/s, *m* = 4.4 ± 1.7 bp, k_{obs} = 90 ± 25 s^{-1}, k_{NP} = 1.7 ± 0.5 s^{-1}. **(B)**. The number of steps *n* determined from global NLLS analysis using Scheme 1 plotted versus DNA duplex length *L*. The solid line shows the linear least squares fit through the data ($n = 0.23L + 0.03$).

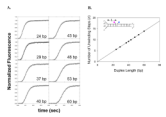

Figure 5.

Single-turnover kinetics of RecBC catalyzed unwinding of DNA duplexes possessing non-complementary 5'-$(dT)_6$ and 3'-$(dT)_6$ ssDNA tails using the stopped-flow fluorescence assay. **(A)**. Cy3 fluorescence time courses as a function of duplex length (L = 24, 29, 37, 40, 43, 48, 53, and 60 bp). Data points represent the average of three independent measurements and the error bars indicate the standard deviation of the data. Smooth curves are simulated time courses based on the global NLLS best fits to Scheme 1, with: mk_{obs} = 348 ± 5 bp/s, m = 4.4 ± 0.1 bp, k_{obs} = 79 ± 11 s^{-1}, k_{NP} = 1.1 ± 0.1 s^{-1}. **(B)**. The number of unwinding steps n determined from the global NLLS analysis using Scheme 1 plotted versus DNA duplex length, L. The solid line shows the linear least squares fit through the data ($n = 0.23L - 0.02$).

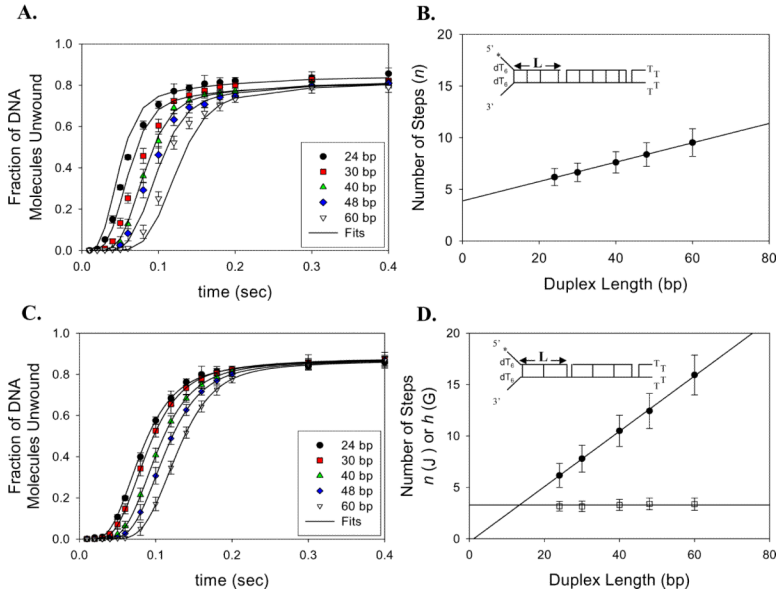

Figure 6.

Single-turnover kinetics of RecBCD catalyzed unwinding of DNA duplexes possessing non-complementary 5'-$(dT)_6$ and 3'-$(dT)_6$ ssDNA tails. **(A).** Time courses as a function of duplex length (L = 24 bp, (J); L = 30 bp, (B); L = 40 bp, (H); L = 48 bp, (F); L = 60 bp, (S)), obtained using the quenched-flow assay. Data points correspond to the average of three independent measurements and the error bars indicated the standard deviation of the data. Smooth curves are simulated time courses based on the global NLLS best fits to Scheme 1, with: mk_U = 410 ± 12 bp/s, m = 10.1 ± 0.9 bp, k_U = 39 ± 23 s^{-1}, k_{NP} = 5.9 ± 1.8 s^{-1}. **(B)**. The number of steps n determined from global NLLS analysis using Scheme 1 plotted versus DNA duplex length L. The solid line shows the linear least squares fit through the data (n = 0.09L + 3.88). **(C).** The same data from panel **(A)** was analyzed using the Scheme 2 which includes the additional kinetic steps with rate constant k_C, which are not involved in DNA unwinding. Smooth curves are simulated time courses based on the global NLLS best fits to Scheme 2, with: mk_U = 774 ± 16 bp/s, m = 3.3 ± 1.3 bp, k_U = 240 ± 56 s^{-1}, k_{NP} = 1.1 ± 0.3 s^{-1}, h = 3.2 ± 0.2 steps, k_C = 45 ± 2 s^{-1}. **(D).** The number of unwinding steps n and additional kinetic steps h determined from global NLLS analysis using Scheme 2 plotted versus DNA duplex length L. The solid line shows the linear least squares fit through the data (n = 0.27L − 0.21; h = 3.3).

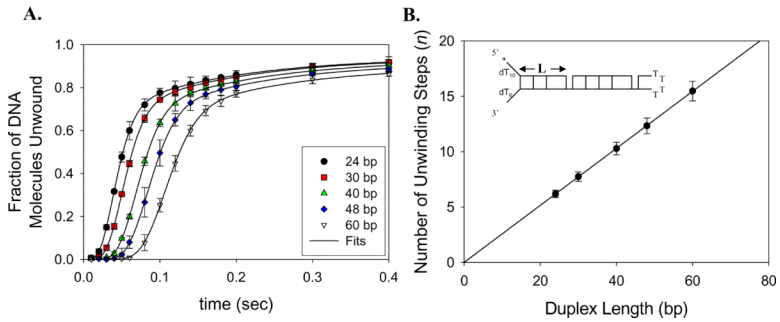

Figure 7.

Single-turnover kinetics of RecBCD catalyzed unwinding of DNA duplexes possessing non-complementary 5'-$(dT)_{10}$ and 3'-$(dT)_6$ ssDNA tails obtained. **(A)**. Timecourses obtained as a function of duplex length (*L* = 24 bp, (J); *L* = 30 bp, (B); *L* = 40 bp, (H); *L* = 48 bp, (F); *L* = 60 bp, (S)) using the chemical quenched-flow assay. Data points represent the average of three independent measurements and the error bars indicate the standard deviation of the data. Smooth curves are simulated time courses based on the global NLLS best fits to Scheme 1, with: mk_U = 538 ± 24 bp/s, *m* = 3.9 ± 0.5 bp, k_U = 138 ± 37 s^{-1}, k_{NP} = 6.7 ± 1.8 s^{-1}. **(B)**. Plot of the number of unwinding steps *n* versus duplex length *L*. The solid line shows the linear least squares fit through the data (*n* = 0.26*L*).

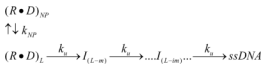

Scheme 1.

Scheme 2.

Table 1

Sequences of DNA unwinding substrates

DNA	Length (nt)*	DNA Sequence of Strand "A"
Ia	24	5'-$(dT)_n$ CCA TGG CTC CTG AGC TAG CTG CA(Cy3) G-3'
IIa	29	5'-$(dT)_n$ CCA TGG CTC CTG AGC TAG CTG CAG TAG C(Cy3)C-3'
IIIa	30	5'-$(dT)_n$ CCA TGG CTC CTG AGC TAG CTG CAG TAG CC(Cy3) T-3'
IVa	37	5'-$(dT)_n$ CCA TGG CTC CTG AGC TAG CTG CAG TAG CCT AAA GGA (Cy3)T-3'
Va	40	5'-$(dT)_n$ CCA TGG CTC CTG AGC TAG CTG CAG TAG CCT AAA GGA TGA (Cy3)A-3'
VIa	43	5'-$(dT)_n$ CCA TGG CTC CTG AGC TAG CTG CAG TAG CCT AAA GGA TGA AAC (Cy3)T-3'
VIIa	48	5'-$(dT)_n$ CCA TGG CTC CTG AGC TAG CTG CAG TAG CCT AAA GGA TGA AAC TAG GA(Cy3) T-3'
VIIIa	53	5'-$(dT)_n$ CCA TGG CTC CTG AGC TAG CTG CAG TAG CCT AAA GGA TGA AAC TAG GAT CTT A(Cy3) T-3'
IXa	60	5'-$(dT)_n$ CCA TGG CTC CTG AGC TAG CTG CAG TAG CCT AAA GGA TGA AAC TAG GAT CTT ATG CTC CA(Cy3) T-3'

	Length (nt)	DNA sequance of Strand "B"
Ib	56	5'-(Cy5) TAG CCT AAA GGA TGA AAC TAG GAT CTT ATG CTC CAT GGA TAC GTC GAG TCG CAT CC-3'
IIb	51	5'-(Cy5) TAA AGG ATG AAA CTA GGA TCT TAT GCT CCA TGG ATA CGT CGA GTC GCA TCC-3'
IIIb	50	5'-(Cy5) AAA GGA TGA AAC TAG GAT CTT ATG CTC CAT GGA TAC GTC GAG TCG CAT CC-3'
IVb	43	5'-(Cy5) GAA ACT AGG ATC TTA TGC TCC ATG GAT ACG TCG AGT CGC ATC C-3'
Vb	40	5'-(Cy5) ACT AGG ATC TTA TGC TCC ATG GAT ACG TCG AGT CGC ATC C-3'
VIb	37	5'-(Cy5) AGG ATC TTA TGC TCC ATG GAT ACG TCG AGT CGC ATC C-3'
VIIb	32	5'-(Cy5) CTT ATG CTC CAT GGA TAC GTC GAG TCG CAT CC-3'
VIIIb	27	5'-(Cy5) GCT CCA TGG ATA CGT CGA GTC GCA TCC-3'
IXb	20	5'-(Cy5) GGA TAC GTC GAG TCG CAT CC-3'

Hp	Length (nt)	DNA Sequence of Strand "Hp"
	120	5'-AGA TCC TAG TGC AGG TTT TCC TGC ACT AGG ATC TGG ATG CGA CTC GAC GTA TCC ATG GAG CAT AAG ATC CTA GTT TCA TCC TTT AGG CTA CTG CAG CTA GCT CAG GAG CCA TGG TTTTTT-3'

Substrate I is formed by annealing strands Ia, Ib, and the bottom strand Hp. Substrates II-IX are formed similarly. DNA strands A and B are fluorescently labeled with Cy3 and Cy5, respectively for use in stopped-flow experiments.

*The length of DNA strand A refers to the number of base pairs that will form when annealed with the bottom strand (Hp) and therefore the DNA duplex length that is unwound in the kinetic experiment.

Table 2

Kinetics summary of chemical quenched-flow and stopped-flow fluorescence unwinding results

Quenched-Flow Results

RecBCD	mk_u (bp/sec)	K_u (s^{-1}	m (bp)	k_c (s^{-1})	h (steps)	k_{NP} (s−1)	x
Blunt Ends[41]	790 ± 23	196 ± 77	3.9 ± 1.3	29 ± 3	2.0 ± 0.2	1.1 ± 0.2	0.84 ± 0.02
5′/3′T6	774 ± 16	240 ± 56	3.3 ± 1.3	45 ± 2	3.2 ± 0.2	1.1 ± 0.3	0.89 ± 0.04
5′T10,3′T6	538 ± 24	138 ± 37	3.9 ± 0.5	--	0	6.7 ± 1.8	0.81 ± 0.03

RecBC	mk_{obs} (bp/sec)	k_{obs} (s^{-1})	m (bp)	k_c (s^{-1})	h (steps)	k_{NP} (s^{-1})	
5′/3′ T6	396 ± 15	90 ± 25	4.4 ± 1.7	--	0	1.7 ± 0.5	0.81 ± 0.02
5′T10,3′T6	372 ± 21	103 ± 33	3.6 ± 0.9		0	2.5 ± 1.2	0.80 ± 0.02

Stopped-Flow Results

RecBCD	mk_u (bp/sec)	k_u (s^{-1})	m (bp)	k_c (s^{-1})	h (steps)	k_{NP} (s^{-1})	x
Blunt Ends[48]	680 ± 12	200 ± 40	3.4 ± 0.6	51 ± 5	3.2 ± 0.3	6.0 ± 0.3	0.87 ± 0.01
5′/3′T6	745 ± 18	220 ± 28	3.4 ± 0.5	58 ± 2	3.2 ± 0.1	6.7 ± 0.3	0.83 ± 0.01
5′T10,3′T6	588 ± 11	163 ± 24	3.6 ± 0.2	--	0	5.4 ± 1.0	0.80 ± 0.01

RecBC	mk_{obs} (bp/sec)	k_{obs} (s^{-1})	m (bp)	k_c (s^{-1})	h (steps)	k_{NP} (s^{-1})	
5′/3′T6	348 ± 5	79 ± 11	4.4 ± 0.1	--	0	1.1 ± 0.1	0.79 ± 0.03
5′T10,3′T6	320 ± 7	92 ± 12	3.5 ± 0.1	--	-	1.9 ± 0.6	0.81 ± 0.02

J Mol Biol. Author manuscript; available in PMC 2011 September 16.